journal of the mechanical behavior of biomedical materials 134 (2022) 105339

Contents lists available at ScienceDirect

Journal of the Mechanical Behavior of Biomedical Materials

journal homepage: www.elsevier.com/locate/jmbbm

Time-course of the human thoracic aorta ageing process assessed using uniaxial mechanical testing and constitutive modelling

Alessandro Giudici [a,b], Ye Li [a,c], Yasmin [d], Sarah Cleary [d], Kathleen Connolly [d], Carmel McEniery [d], Ian B. Wilkinson [d], Ashraf W. Khir [a,e,*]

[a] Brunel Institute for Bioengineering, Brunel University London, Kingston Lane, Uxbridge, UB8 3PH, UK
[b] Department of Biomedical Engineering, CARIM School for Cardiovascular Diseases, Maastricht University, 6229 ER, the Netherlands
[c] British Heart Foundation Centre, King's College London, Strand, London, WC2R 2LS, UK
[d] Division of Experimental Medicine and Immunotherapeutics, University of Cambridge, Hills Road, Cambridge, CB2 0QO, UK
[e] Department of Engineering, Durham University, Durham, DH1 3LE, UK

ARTICLE INFO

Keywords:
Aorta
Arterial ageing
Arterial stiffness
Collagen
Elastin
Constitutive modelling

ABSTRACT

Age-related remodelling of the arterial wall shifts the load bearing from the compliant elastin network to the stiffer collagen fibres. While this phenomenon has been widely investigated in animal models, human studies are lacking due to shortage of donors' arteries. This work aimed to characterise the effect of ageing on the mechanical properties of the human aortic wall in the circumferential direction.

N = 127 thoracic aortic rings (age 18–81 years) were subjected to circumferential tensile testing. The tangential elastic modulus ($\mathscr{K}_{\theta\theta\theta\theta}$) was calculated at pressure-equivalent stresses ranging 60–100 mmHg. Further, the mechanical data were fitted using the Holzpafel-Gasser-Ogden hyperelastic strain energy function (HGO-SEF), modelling the superimposed response of an isotropic matrix (elastin) reinforced by collagen fibres.

$\mathscr{K}_{\theta\theta\theta\theta}$ increased with age across at all considered pressures ($p < 0.001$), although more strongly at higher pressures. Indeed, the slope of the linear $\mathscr{K}_{\theta\theta\theta\theta}$-pressure relationship increased by 300% from donors <30 to ≥70 years (4.72± 2.95 to 19.06± 6.82 kPa/mmHg, $p < 0.001$). The HGO-SEF elastin stiffness-like parameter dropped by 31% between 30 and 40 years ($p < 0.05$) with non-significant changes thereafter. Conversely, changes in HGO-SEF collagen parameters were observed later at age>60 years, with the exponential constant increasing by ~20–50 times in the investigated age range ($p < 0.001$).

The results provided evidence that the human thoracic aorta undergoes stiffening during its life-course. Constitutive modelling suggested that these changes in arterial mechanics are related to the different degeneration time-courses of elastin and collagen; likely due to considerable fragmentation of elastin first, with the load bearing shifting from the compliant elastin to the stiffer collagen fibres. This process leads to a gradual impairment of the aortic elastic function with age.

1. Introduction

Collagen and elastin are the two main structural proteins determining the passive mechanical properties of conduit arteries. The compliant elastin network allows arteries to dilate and take in blood during systolic ejection, and to recoil during diastole, maintaining flow. Stiffer collagen fibres work as a protective structural element against high pressure levels, preventing mechanical damage to the tissue (Burton, 1954; Wolinsky and Glagov, 1964). Collagen fibres are wavy at low pressure levels, and gradually straighten with increasing pressure. This pressure-dependent structural transition is responsible for the non-linear stress-strain relationship of the arterial wall, whereas the fibres' preferential orientation determines its level of anisotropy (Fonck et al., 2007; Krasny et al., 2017).

Ageing has important consequences on the macro- and microstructure of human arteries, involving all constituents that determine their mechanical response. Smooth muscle cells migrate from the media, where they are substituted by collagen fibres, to the intima, where they proliferate, thus generating a considerable intimal thickening (Graham et al., 2011; Harvey et al., 2016; Tesauro et al., 2017). Further, the elastin network, undergoing very limited turnover *in vivo*, becomes

* Corresponding author. Department of Engineering, Durham University, Lower Mountjoy, South Road, Durham, DH1 3LE, UK.
E-mail address: ashraf.w.khir@durham.ac.uk (A.W. Khir).

https://doi.org/10.1016/j.jmbbm.2022.105339
Received 7 March 2022; Received in revised form 18 June 2022; Accepted 25 June 2022
Available online 4 July 2022

Abbreviations:

h0	undeformed wall thickness
λ_θ	circumferential stretch
D0	undeformed diameter
λ_z	axial stretch
w0	undeformed wall width
$\mathscr{K}_{\theta\theta\theta\theta}$	tangential elastic modulus
d	diameter of the tensiometer holding pin
$\dot{\mathscr{K}}_{\theta\theta\theta\theta}$	slope of the tangential elastic moduls-pressure relationship
P	luminal pressure
F	force applied by the tensiometer
Ψ	strain energy function
L0	inter-pin distance at rest (no load applied)
μ	elastin stiffness-like parameter
L	inter-pin distance when a load is applied
k1	collagen stiffness-like parameter
$\varepsilon_{\theta\theta}$	circumferential strain
k2	collagen non-linearity parameter
$t_{\theta\theta_{\mathrm{exp}}}$	experimental circumferential Cauchy stress
α	principal orientation of the collagen fibres
$t_{\theta\theta_{\mathrm{mod}}}$	modelled circumferential Cauchy stress
ρ	collagen fibre dispersion parameter

sparser and fragmented, thus losing its functionality (Greenwald, 2007; Harvey et al., 2016; Kohn et al., 2015). On the other hand, collagen crosslinking increases with age, as does its degree of alignment (Haskett et al., 2010; Kohn et al., 2015; Tsamis et al., 2013), making its role more dominant in managing the pressure pulse. Furthermore, structural remodelling is accompanied also by changes in the wall composition; collagen volume fraction rises with age, while those of elastin and smooth muscle cells decrease (Greenwald, 2007; Spina et al., 1983; Tsamis et al., 2013). Since the elastin content remains unchanged, these changes have to be attributed to enhanced synthesis of collagen fibres (Graham et al., 2010; Harvey et al., 2016; Spina et al., 1983; Tesauro et al., 2017; Tsamis et al., 2013).

These structural changes result in a gradual stiffening of the arterial wall with age. Although arterial stiffness, defined as the tangential elastic modulus (i.e., the tangent to the stress-strain curve) is intrinsically pressure-dependent and cannot, thus be defined in absolute terms (Giudici et al., 2021), the circumferential tangential elastic modulus of the thoracic aorta at mean arterial pressure (100 mmHg) more than doubles across the life-span of an individual (Haskett et al., 2010; Jadidi et al., 2020). Further, consistently with the development of a highly collagenous tissue (Fonck et al., 2007; Gundiah et al., 2013), ageing enhances the nonlinearity of the behaviour of elastic arteries, increasing the sensitivity of their stiffness to pressure (Learoyd and Taylor, 1966).

The overall objective of this study was to further our understanding of how age-related remodelling of the aortic wall affects the stiffness of the healthy human thoracic aorta. First, we aimed to provide reference values of the wall tangential elastic modulus in the circumferential direction, which is most relevant to the pulsatile blood flow. Second, we sought to characterise the pressure-dependence of arterial stiffness in relation to aging and its consequent remodelling. Further, using constitutive modelling of the aortic wall, this study aimed to provide a microstructural interpretation of the experimental data, providing insights into the time course of wall remodelling by discerning the alterations in structural and mechanical properties of elastin and collagen, and evaluating consequences on arterial function.

2. Materials and methods

2.1. Arterial samples

Aortae obtained from 127 human organ donors following Research Ethics Committee (REC) and family consent were stored at −80 °C. A 10 mm wide ring was cut from each aorta in the descending thoracic region (i.e., downstream to the aortic arch and above the diaphragm). The connective tissues surrounding the ring sample was carefully removed and the absence of atherosclerotic plaques, calcification and side branches was verified before testing. Unloaded wall thickness (h_0), ring internal diameter (D_0) and width (w_0) were measured using a digital calliper.

2.2. Mechanical testing

Aortic rings underwent uniaxial tensile testing (i.e., ring test). Each ring was mounted on an Instron (Norwood, MA, USA) tensile device equipped with a 100 N load cell and tissue holder suitable for ring tests. The diameter of each holding pin d was 5 mm. The ring was first preloaded at 0.05 N to ensure that the two sides of the ring were parallel to the loading direction, then tested according to a previously reported protocol (calf aortas in Li et al., 2021): 1) cycled three times between 0 and 30 mmHg equivalent force, 2) cycled three times between 30 and 80 mmHg equivalent force, and 3) cycled three times between 15 and 100 mmHg equivalent force at a speed of 10 mm/min. This deformation speed was chosen to minimise viscoelastic effects (Franchini et al., 2021; Jadidi et al., 2020). For each sample, the pressure-equivalent load was estimated as previously reported (Burton, 1954):

$$F = PD_0w_0\ , \tag{1}$$

where F is the force applied by the tensile device and P is the corresponding arterial pressure. The loading phase of the last load cycle from 15 to 100 mmHg was considered for the analysis. Samples were kept wet throughout the test by spraying saline solution. All tests were conducted twice and reported data are the average of both tests.

2.3. Data analysis

The deformation induced by a ring test is generally non-trivial; e.g., the entity of the circumferential deformation is dependent on the radial coordinate. However, as proposed by Cox (1983), the circumferential strain can be approximated to that at the luminal surface:

$$\varepsilon_{\theta\theta} = \lambda_\theta - 1 = \frac{2L + \pi d}{2L_0 + \pi d} - 1 = \frac{L - L_0}{L_0 + \pi d/2}\ , \tag{2}$$

where λ_θ is the circumferential stretch, L is the loaded sample inter-pin distance and L_0 is the undeformed sample inter-pin distance.

The experimental circumferential Cauchy stress ($t_{\theta\theta_{\mathrm{exp}}}$) was calculated as:

$$t_{\theta\theta_{\mathrm{exp}}} = \frac{F}{A} = \frac{F}{A_0}\lambda_\theta = \frac{F}{2h_0w_0}\lambda_\theta\ , \tag{3}$$

where A is the deformed cross-sectional area. Note: 2 in the denominator of Eq. (3) pertains two sides of the ring being tested.

The tangential elastic modulus was calculated as

$$\mathscr{K}_{\theta\theta\theta\theta} = \left.\frac{\partial t_{\theta\theta_{\mathrm{exp}}}}{\partial \varepsilon_{\theta\theta}}\right|_{P=P_{\mathrm{ref}}}\ , \tag{4}$$

indicating the tangent to the circumferential Cauchy stress-circumferential strain relationship at the stress level equivalent to the pressure P_{ref}, which can be determined using the Laplace equation

$$P_{\text{ref}} = \frac{t_{\theta\theta} h}{R}, \tag{5}$$

where R and h are the deformed ring radius and wall thickness, respectively. While R can easily be determined as $R = R_0\lambda_\theta$, changes in wall thickness were not measured throughout the test. Hence, h was approximated with the undeformed thickness h_0, so that Eq. (5) is rewritten as

$$P_{\text{ref}} \approx \frac{t_{\theta\theta} h_0}{R_0 \lambda_\theta}. \tag{6}$$

The tangential elastic modulus, $\mathscr{K}_{\theta\theta\theta\theta}$, was calculated for $P_{\text{ref}} =$ 60, 80, and 100 mmHg.

The stress-strain relationship of arteries is approximately exponential in the physiological range of pressures as demonstrated in earlier studies (Bergel, 1961; Burton, 1954; Giudici et al., 2021). This yields a nearly linear $\mathscr{K}_{\theta\theta\theta\theta}$-$P$ relationship, with its slope quantifying the pressure-induced arterial stiffening. To characterise changes in this relationship with age, we calculated $\dot{\mathscr{K}}_{\theta\theta\theta\theta}$ as the slope of the linear regression between $\mathscr{K}_{\theta\theta\theta\theta}$ and P for $P_{\text{ref}} =$ 60, 80, and 100 mmHg:

$$\dot{\mathscr{K}}_{\theta\theta\theta\theta} = \frac{\mathrm{d}\mathscr{K}_{\theta\theta\theta\theta}}{\mathrm{d}P}. \tag{7}$$

2.4. Constitutive modelling

Determination of $\mathscr{K}_{\theta\theta\theta\theta}$ and $\dot{\mathscr{K}}_{\theta\theta\theta\theta}$ allows evaluating the effects that age-related arterial remodelling has on the mechanical properties of the arterial wall as a whole. However, it does not provide insight into the microstructural changes that are at their basis. Structurally-motivated constitutive models are mathematical descriptions of the wall behaviour that account for the mechanical contribution of its constituents. Therefore, fitting the model parameters on mechanical data can provide insight into age-related constituent-specific remodelling determining the observed changes in the macroscopic wall behaviour.

In this study, the human thoracic aorta was modelled as a thin cylindrical membrane as done in previous studies (Jadidi et al., 2020; Weisbecker et al., 2012). This entails calculating average stresses and stretches values through the wall thickness and neglecting the effect of residual stresses on the distribution of stresses across the wall thickness (Holzapfel and Ogden, 2010; Saini et al., 1995). The behaviour of the human thoracic aortic wall was modelled using the Holzapfel-Gasser-Ogden (HGO) hyperelastic strain energy function (SEF; Ψ) (Gasser et al., 2006), which accounts for the contribution of an isotropic matrix (typically associated with elastin) reinforced by two symmetrically-oriented families of fibres (collagen).

$$\Psi = \mu(I_1 - 3) + \sum_{i=1}^{2} \frac{k_1}{2k_2}\left(e^{k_2\left[\rho(I_1)+(1-3\rho)I_{4,i}-1\right]^2} - 1\right), \tag{8}$$

where μ is the isotropic matrix stiffness-like parameter, k_1 is the fibre stiffness-like parameter, k_2 is the fibre nonlinearity parameter, and $\rho \in \left[0, \frac{1}{3}\right]$ is the fibre dispersion parameter. $I_1 = \lambda_\theta^2 + \lambda_z^2 + 1/(\lambda_\theta^2\lambda_z^2)$ (λ_z quantifies the sample deformation in the axial direction) and $I_{4,i} = \lambda_\theta^2 \cos^2(\alpha_i) + \lambda_z^2 \sin^2(\alpha_i)$ are the first and fourth invariant of the Cauchy-Green tensor, respectively, and $i = \{1, 2\}$ indicates the two symmetrically oriented collagen fibres: $\alpha_{1,2} = \{\alpha, -\alpha\}$. Given Eq. (8), the modelled Cauchy stress can be calculated as

$$t_{\theta\theta_{\text{mod}}} = -p + 2\lambda_\theta^2 \frac{\partial \Psi}{\partial \lambda_\theta^2}, \tag{9}$$

where p is the Lagrange multiplier enforcing incompressibility. Note that, from Eq. (8) and Eq. (9), the determination of $t_{\theta\theta_{\text{mod}}}$ requires knowledge of the deformation in both λ_θ and λ_z. While λ_θ was calculated using Eq. (2), λ_z was not measured during the ring tests but was estimated by imposing the axial stress $t_{zz} = 0$ (i.e., the arterial wall is loaded only in the circumferential direction) and enforcing incompressibility.

The model parameters were determined by minimising the cost function Π corresponding to the error between the modelled and experimental stresses:

$$\Pi = \sum \left(t_{\theta\theta_{\text{mod}}} - t_{\theta\theta_{\text{exp}}}\right)^2. \tag{10}$$

The absence of experimental data in the axial direction does not allow the evaluation of the degree of anisotropy of the tissue which, from the constitutive modelling perspective, is determined by the fibre orientation and dispersion parameters α and ρ, respectively. To avoid overfitting (Supplementary Fig. S1), α and ρ were fixed to values previously reported in the literature. Using a similar model Haskett et al. (2010) found that the fibre orientation shifted towards the axial direction with progressing age, in agreement with findings reported by Weisbecker et al. (2012) in older adults. Therefore, α was set to 44.5° for people <60 years and 50.0° in older adults (Haskett et al., 2010; Weisbecker et al., 2012). Similarly, ρ was set to 0.10 for young arteries (donor's age <30 years) and 0.20 for middle-aged and older donors (Haskett et al., 2010; Weisbecker et al., 2012). Further, since imposing stepwise changes to α and ρ could possibly lead to abrupt variation of the fitted μ, k_1 and k_2 with age, parameters were also estimated assuming age-independent $\alpha =$ 44.5° and $\rho =$ 0.20. We also conducted a preliminary analysis of our experimental data to confirm that all three remaining unconstrained model parameters (i.e., μ, k_1 and k_2) were necessary to obtain a good fit of the non-linear experimental curves (Supplementary Fig. S2).

Finally, the ability of the thoracic aorta to store elastic energy during systole was evaluated as the difference between the HGO-SEF Ψ (Eq. (8)) at 100 and 80 mmHg (Spronck et al., 2020):

$$\Delta\Psi = \Psi|_{100\ \text{mmHg}} - \Psi|_{80\ \text{mmHg}}, \tag{11}$$

2.5. Statistical analysis

The statistical analysis was carried out using SPSS 23 (IBM corporation, Chicago, IL, USA), considering age both as a continuous and as a categorical variable by grouping samples in decade age-groups (Table 1). Younger than 30 and older than 70 years were grouped as <30 and ≥70 years, respectively, due to their limited numbers. Differences between age groups were first evaluated using analysis of covariance (ANCOVA) test with sex as confounder, followed by post-hoc pairwise comparisons when statistical significance was reached. Further, Pearson's test has been used to evaluate the correlation between age and biomechanical variables where appropriate, and a multivariate regression model was used to evaluate the effect of gender, age, body weight and height on the unloaded aortic radius and wall thickness.

Data in tables are presented as mean ± standard deviation. The

Table 1
Age, sex, and ring size in the 6 age groups.

Age group [years]	<30	30–39	40–49	50–59	60–69	>70
Men: women [N]	11 : 0	5 : 5	20 : 6	22 : 14	15 : 15	5 : 9
Age [years]	23 ± 4	34 ± 3	46 ± 2	55 ± 3	63 ± 3	74 ± 4
Body weight [kg]	81.1 ± 11.8	76.2 ± 10.0	84.3 ± 13.3	81.9 ± 18.8	77.5 ± 13.5	75.8 ± 13.8
Body height [m]	1.83 ± 0.08	1.73 ± 0.11	1.72 ± 0.09	1.70 ± 0.08	1.70 ± 0.09	1.66 ± 0.10
R_0 [mm]	5.80 ± 0.52	6.19 ± 0.48	6.61 ± 0.87	7.33 ± 1.24	7.62 ± 1.15	8.99 ± 1.69
h_0 [mm]	1.14 ± 0.26	1.32 ± 0.18	1.30 ± 0.23	1.46 ± 0.26	1.52 ± 0.27	1.62 ± 0.29

R_0: unloaded internal radius; h_0: unloaded wall thickness. Data are presented as mean ± standard deviation.

average curves have been built by averaging the stress-strain and pressure-diameter relationships of the subjects in each age group. $p < 0.05$ has been taken as statistical significance.

3. Results

3.1. Donors' demographic and mechanical testing

Donor demographics can be seen in Table 1. All age groups except <30 years and 40–49 years presented an even distribution of men and women. Under 30 years there were men only and 40–49 years there were more men (77%). There was a significant increase in both the unloaded aortic diameter ($r = 0.70$, $p < 0.001$) and wall thickness with age ($r = 0.37$, $p < 0.001$). The multivariate regression analysis indicated that age and height were significantly associated with the unloaded aortic diameter (β =0.78, $p < 0.0001$ and $\beta = 0.37$, $p < 0.0001$, respectively), while no significant associations other than age was found for the unloaded wall thickness.

The average pressure-diameter and circumferential Cauchy stress-stretch relationships are shown in Fig. 1. The increase in diameter with age can clearly be observed in Fig. 1A where pressure-diameter relationships shift rightward with progressing age, as did the stress-stretch relationships, requiring, on average, a higher level of stretch to reach a given level of wall stress. Indeed, λ_θ at 80 kPa of Cauchy stress, representative of the wall circumferential stress *in vivo* (Franchini et al., 2021; Peña et al., 2015), was significantly lower at 1.35 ± 0.05 in <30 years rings than rings harvested from middle-aged donors (1.43± 0.05, 1.42± 0.05, and 1.43± 0.05 in 30–39, 40–49, and 50–59 years, respectively, $p < 0.05$). Up to 50–59 years, the average stress-stretch relationships in all age groups were below that of the youngest age group, which crossed the curve of the oldest age group only at $\lambda_\theta = \sim 1.32$.

Fig. 2 presents $\mathcal{K}_{\theta\theta\theta\theta}$ calculated at the pressure-equivalent stress levels of 60 and 100 mmHg as a function of age. Age-group averages are reported in Table 2. Age-differences in wall stiffness ($\mathcal{K}_{\theta\theta\theta\theta}$) were more accentuated at mean pressure (100 mmHg) than at low physiological pressure (60 mmHg). At 100 mmHg, $\mathcal{K}_{\theta\theta\theta\theta}$ was 0.55 ± 0.16 MPa in donors below 30 years. Despite already rising on average by ~33% at 50–59 years, changes in $\mathcal{K}_{\theta\theta\theta\theta}$ at 100 mmHg were significant only at 60–69 years and ≥ 70 years, when $\mathcal{K}_{\theta\theta\theta\theta}$ nearly tripled compared to <30 years (+157%). On the contrary, $\mathcal{K}_{\theta\theta\theta\theta}$ at 60 mmHg was 0.36 ± 0.06 MPa in donors <30 years, significantly different only than that in arteries above 70 years (80% increase).

As expected, $\mathcal{K}_{\theta\theta\theta\theta}$ increased linearly with pressure (average $r \geq 0.95$, $p < 0.001$ for all age-groups) (Fig. 3A), reflecting the exponential nature of the stress-stretch relationship of arteries (Fig. 1B). The pressure-related arterial stiffening $\dot{\mathcal{K}}_{\theta\theta\theta\theta}$, corresponding to the slope of the linear $\mathcal{K}_{\theta\theta\theta\theta}$-$P$ relationship in Fig. 3A, was 4.72 ± 2.95 kPa/mmHg in young donors and approximately four times higher at 19.06 ± 6.82 kPa/mmHg in older adults (≥ 70 years), signifying an enhanced sensitivity to pressure changes (Fig. 3B). This result implies that, in agreement with Fig. 2, the higher the pressure level the more pronounced are age-related differences in $\mathcal{K}_{\theta\theta\theta\theta}$. Furthermore, changes in $\dot{\mathcal{K}}_{\theta\theta\theta\theta}$ appeared relatively small before 50 years of age, followed by a steep increase in middle-aged and older adults.

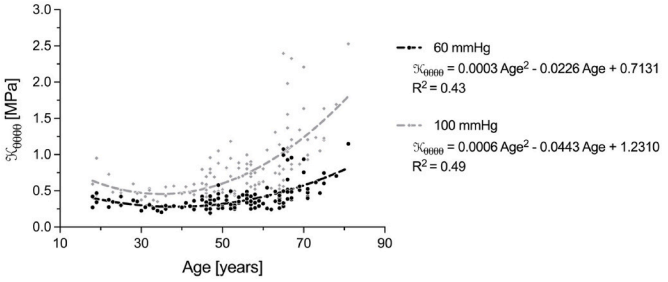

Fig. 2. Changes with age of the tangential elastic modulus $\mathcal{K}_{\theta\theta\theta\theta}$ of the thoracic aorta at the luminal pressure of 60 and 100 mmHg. Note that stiffening with increasing pressure is observed across all ages, although more accentuated in older individuals.

3.2. Constitutive modelling

3.2.1. Age-dependent anisotropy parameters

Constitutive modelling of the arterial wall behaviour was used to provide a plausible microstructural interpretation of the age-related changes observed in the mechanical data. Fig. 4 presents trends of the constitutive model parameters with age when α and ρ were assumed to be age-dependent. Their age-group averages are presented in Table 3 (top). The matrix stiffness-like parameter μ showed a decreasing trend that resembled a quadratic function (Panel A, $R^2 = 0.26$), ranging from 15.94 ± 3.96 kPa in young donors (<30 years) to 8.31 ± 2.88 kPa after 70 years. Age-group ANCOVA analysis indicated that μ dropped by 31% (0%–59%) between <30 and 30–39 years ($p = 0.057$) and did not change thereafter. The collagen fibre stiffness-like parameter k_1 quadratically increased with age (Panel B, $R^2 = 0.23$, $p < 0.01$) from 99.44 ± 27.14 kPa in <30 to 197.77 ± 92.70 kPa in ≥ 70 years and was significantly different from <30 years only for 60–69 years and older people. The fibre exponential constant k_2 grew exponentially from 2.88 ± 5.43 in people <30 years to more than 20-times as much after 70 years (55.43± 26.03) ($R^2 = 0.56$). Changes in k_2 were significant only after 60 years ($p < 0.01$).

3.3.1. Age-independent anisotropy parameters

Interestingly, assigning age-dependent values to α and ρ only mildly affected the trends of μ and k_2 with age (Fig. 5A and C). Their age-group averages are presented in Table 3 (bottom). μ fell quadratically with age

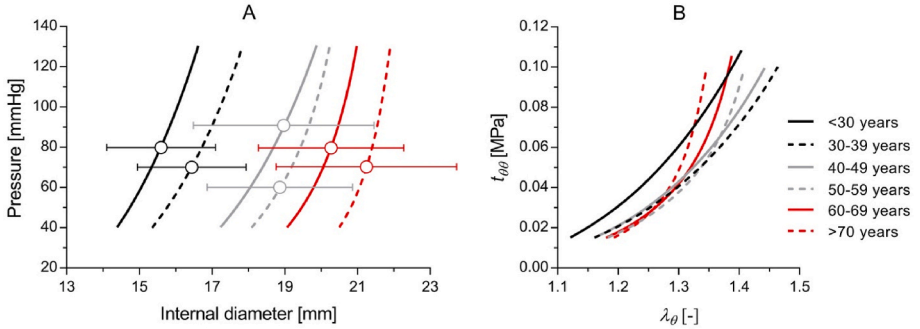

Fig. 1. Average experimental pressure-diameter (A) and Cauchy stress-stretch (B) relationship of the human thoracic aorta in each of the six age groups considered in this study. Pressure was calculated from the circumferential Cauchy stress data using the approximated Laplace equation reported in the Methods (Eq. (6)). Standard deviation bars were not included in panel B for clarity.

Table 2
Tangential elastic modulus ($\mathscr{K}_{\theta\theta\theta\theta}$) of the human thoracic aorta at 60, 80, and 100 mmHg *of pressure-equivalent Cauchy stress for the 6 age-groups included in this study.*

Age group [years]		<30	30–39	40–49	50–59	60–69	>70
$\mathscr{K}_{\theta\theta\theta\theta}$ at	60 mmHg [MPa]	0.36 ± 0.06 ***	0.27 ± 0.04*** ††	0.33 ± 0.10*** ††	0.36 ± 0.13*** †	0.47 ± 0.20**	0.64 ± 0.20
	80 mmHg [MPa]	0.43 ± 0.08 *** †††	0.35 ± 0.06*** †††	0.44 ± 0.15*** †††	0.52 ± 0.22*** ††	0.71 ± 0.29***	1.03 ± 0.35
	100 mmHg [MPa]	0.55 ± 0.16*** †††	0.44 ± 0.09*** †††	0.59 ± 0.22*** †††	0.73 ± 0.34*** †	0.97 ± 0.43***	1.41 ± 0.46

Post-hoc pairwise comparison between age-groups after sex adjustments: *$p < 0.05$, **$p < 0.01$ and ***$p < 0.001$ with ≥ 70 years; †$p < 0.05$, ††$p < 0.01$ and †††$p < 0.001$ with 60–69 years. Data are presented as mean ± standard deviation.

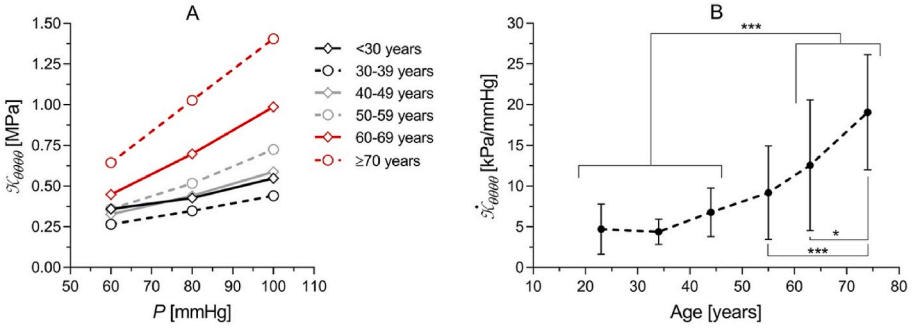

Fig. 3. Changes with age of the pressure-dependence of the tangential elastic modulus of the human thoracic aorta. Panel A: $\mathscr{K}_{\theta\theta\theta\theta}$ as a function of pressure for all the age-groups included in the study (see Table 2 for SD). $\mathscr{K}_{\theta\theta\theta\theta}$ increases with both age and pressure. Panel B: the slope of the $\mathscr{K}_{\theta\theta\theta\theta}$-pressure relationship $\dot{\mathscr{K}}_{\theta\theta\theta\theta}$ indicate the elastic modulus sensitivity to changes in intraluminal pressure, which shows a consitenet incease from the fourth decade onwards. Data are presented as mean ± standard deviation of decade age-groups (except data > 30 and < 70 years that are pooled). *$p < 0.05$ and ***$p < 0.001$.

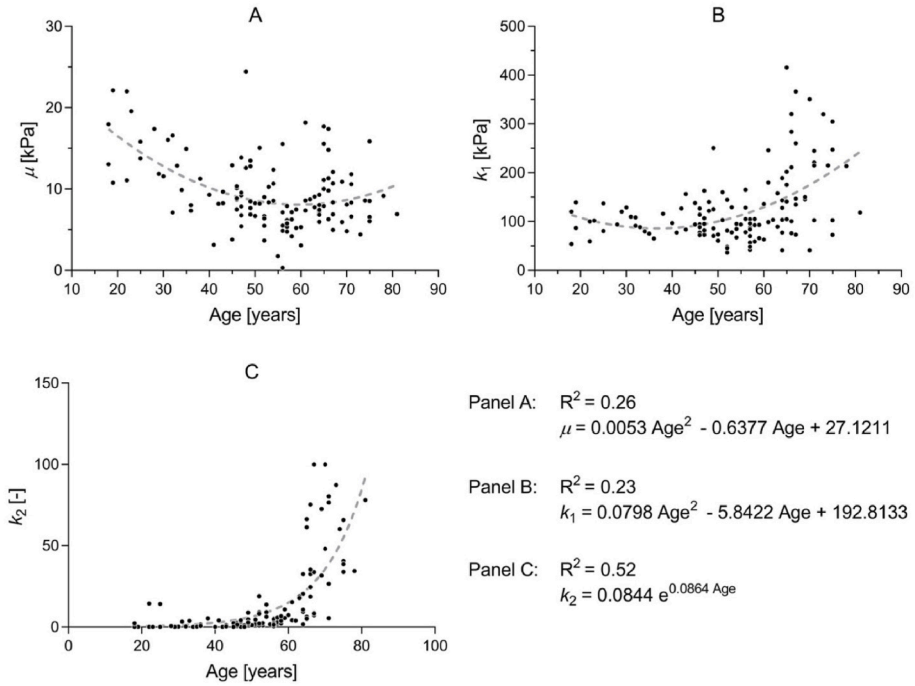

Fig. 4. HGO-SEF model parameters as a function of age; elastin/matrix stiffness-like parameter μ (A), collagen fibre stiffness-like k_1 (B) and exponential k_2 (C) parameters. Anisotropy parameters were assigned age-dependent values taken from the literature, as detailed in the Methods. Dashed lines represent the best-fit functions: quadratic for both μ and k_1, and exponential for k_2.

($R^2 = 0.34$), ranging from 16.37 ± 4.12 kPa in young donors (<30 years) to 6.93 ± 2.56 after 70 years. Age-groups ANCOVA analysis indicated that μ dropped by 31% (2%–60%) between <30 and 30–39 years ($p < 0.05$) and did not change thereafter. k_2 grew exponentially from 0.61 ± 1.84 in people <30 years to more than 50-times as much after 70 years (34.74± 18.06) ($R^2 = 0.42$). On the contrary, k_1, that quadratically increased with age when assuming age-dependent α and ρ, k_1 showed a mild decreasing trend with age (Panel B, $r = -0.24$, $p < 0.01$), falling from 143.63 ± 42.92 kPa to 95.92 ± 43.84 kPa across the investigated age-range, and was significantly different from <30 years only for 50–59 years and older people.

Finally, Fig. 6 shows changes in stored elastic energy over the pressure range 100–80 mmHg. The modelling choices on α and ρ only slightly affected $\Delta\Psi_{100-80\ \mathrm{mmHg}}$ that was 2.32 ± 0.74 kPa in rings <30 years, did not change significantly in the first four decades analysed in this study, and started decreasing by the age of ~60 years reaching 1.03 ± 0.52 kPa after 70 years ($p < 0.001$).

Table 3
Age-group-specific model parameters of the human thoracic aorta. The top part of the table reports model parameters obtained when setting α and ρ to 44.5° and 0.20, respectively, independently on the age-group. The bottom part of the table displays results when using age-dependent α and ρ as detailed in the Methods.

Age group [years]		<30	30–39	40–49	50–59	60–69	>70
Age-dependent α and ρ	μ [kPa]	15.94 ± 3.96	11.56 ± 3.34	9.56 ± 3.98 ***	7.31 ± 3.36 *** †	9.30 ± 3.66 ***	8.31 ± 2.88 ***
	k_1 [kPa]	99.44 ± 27.14 #	93.00 ± 20.87 ‡ ##	110.06 ± 38.70 ‡ ##	88.94 ± 33.67 ‡‡‡ ##	162.99 ± 89.81	197.77 ± 92.70
	k_2 [-]	2.88 ± 5.43 ‡‡ ##	1.54 ± 1.80 ‡‡ ##	1.73 ± 2.02 ‡‡‡ ##	6.25 ± 10.09 ‡‡‡ ##	22.89 ± 24.51 ##	55.43 ± 26.03
Age-independent α and ρ	μ [kPa]	16.37 ± 4.12	11.56 ± 3.34 *	9.56 ± 3.98 ***	7.31 ± 3.36 *** †	7.47 ± 3.06 *** †	6.93 ± 2.56 *** †
	k_1 [kPa]	143.63 ± 42.92	93.00 ± 20.87 *	110.06 ± 38.70	88.94 ± 33.67 ***	93.36 ± 42.79 **	95.92 ± 43.84 *
	k_2 [-]	0.61 ± 1.84 ‡‡ ##	1.54 ± 1.80 ‡ ##	1.73 ± 2.02 ‡‡‡ ##	6.25 ± 10.09 ‡ ##	14.46 ± 15.00 ##	34.74 ± 18.06

Post-hoc pairwise comparison between age-groups after sex adjustments: $^{*}p < 0.05$, $^{**}p < 0.01$ and $^{***}p < 0.001$ with <30 years; $^{\dagger}p < 0.05$ with 30–39 years; $^{\ddagger}p < 0.05$, $^{\ddagger\ddagger}p < 0.01$ and $^{\ddagger\ddagger\ddagger}p < 0.001$ with 60–69 years; $^{\#}p < 0.01$ and $^{\#\#}p < 0.001$ with ≥ 70 years. Data are presented as mean ± standard deviation.

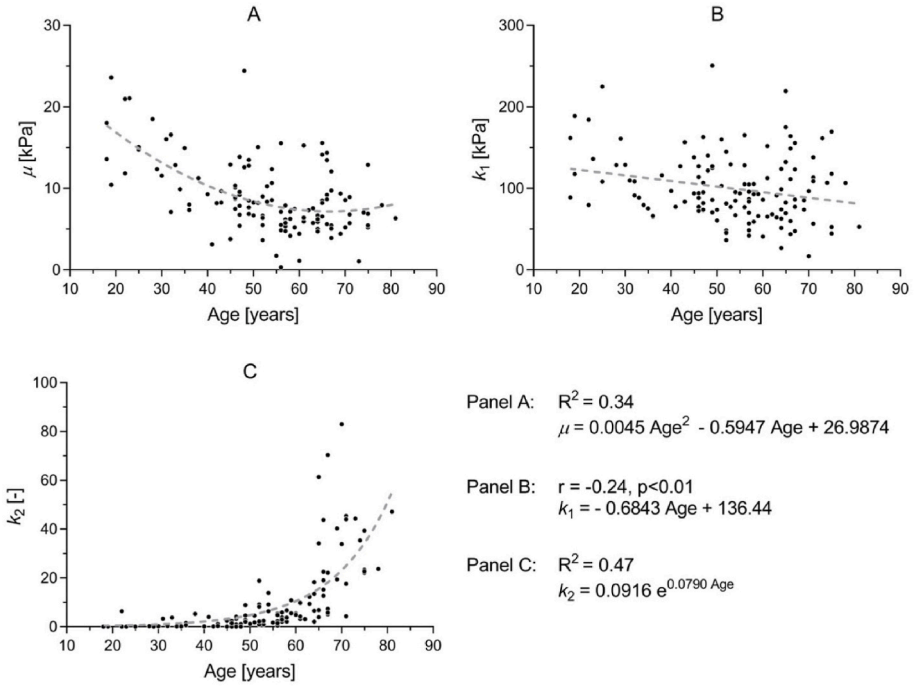

Fig. 5. HGO-SEF model parameters as a function of age; elastin/matrix stiffness-like parameter μ (A), collagen fibre stiffness-like k_1 (B) and exponential k_2 (C) parameters. Anisotropy parameters were assumed constant with age: $\alpha = 44.5°$ and $\rho = 0.20$. Dashed lines represent the best-fit functions: quadratic, linear, and exponential, for μ, k_1 and k_2, respectively.

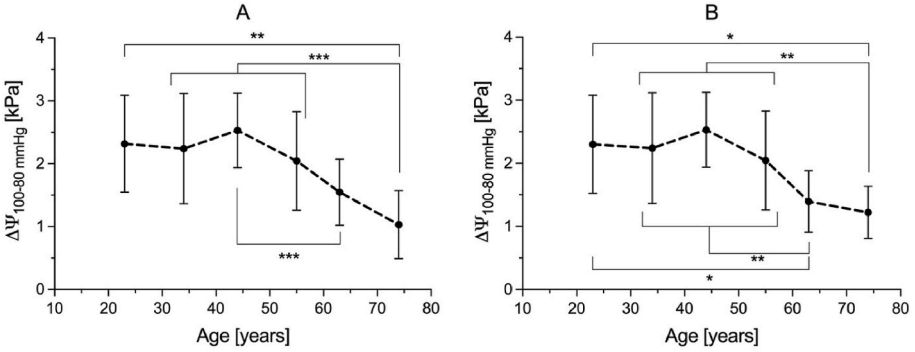

Fig. 6. Changes in stored elastic energy over the pressure range 120-80 mmHg with age. Panel A: α and ρ were assumed independent of age. Panel B: α and ρ were given age-group-specific values as detailed in the methods. Note the nearly constant $\Delta\Psi$ for age up to 5th decade and steady consistent decrease indicating inability to store elastic energy for samples of older donors. Data are presented as mean ± standard deviation. $^{*}p < 0.05$, $^{**}p < 0.01$, $^{***}p < 0.001$.

4. Discussion

The strong relationship between arterial structure and function has long been known (Burton, 1954). Therefore, it is not surprising that structural alterations associated with the ageing process of large arteries affect their mechanical properties. In this study we experimentally evaluated changes of the mechanical properties of the thoracic aorta with age in the circumferential direction *ex vivo* in a large human cohort

(n = 127). Further, using constitutive modelling of the wall behaviour, we provided a microstructural interpretation of the experimental data, inferring changes in the mechanical behaviour of the two main wall constituents: elastin and collagen fibres.

Values of tangential elastic modulus at the mean physiological pressure of 100 mmHg measured in this study are in agreement with those reported previously for the descending thoracic aorta of humans, ranging from ~ 0.4-0.5 MPa in young people (<30 years) to ~ 0.8–1.8 MPa in older adults (>60 years) (Haskett et al., 2010; Jadidi et al., 2020). Interestingly, although $\mathscr{K}_{\theta\theta\theta\theta}$ significantly correlated with age at all pressure levels, the onset of age-related arterial stiffening was not the same for all considered pressure levels: 60–69 years at both $P_{\mathrm{ref}} =$ 80 and 100 mmHg, but older at ≥ 70 years when $P_{\mathrm{ref}} = 60$ mmHg (Figs. 2 and 3A, and Table 2). This different response is also apparent in Fig. 2; while at mean physiological pressure (100 mmHg) $\mathscr{K}_{\theta\theta\theta\theta}$ increased by ~2.5 folds across the investigated age-range, $\mathscr{K}_{\theta\theta\theta\theta}$ at 60 mmHg was much less affected by ageing. Indeed, the slope of the $\mathscr{K}_{\theta\theta\theta\theta}$-$P$ relationship ($\dot{\mathscr{K}}_{\theta\theta\theta\theta}$) increased by 300% across the investigated age range, suggesting that, in line with the development of a highly collagenous tissue (Fonck et al., 2007), elevated pressure levels accelerate the onset of aortic stiffening, with potential implications for untreated hypertensive patients.

To further quantify structural changes in the arterial wall, we fitted the experimental Cauchy stress-stretch relationships with the HGO-SEF which models the superimposed contributions of a compliant isotropic matrix, commonly associated with elastin, and an anisotropic fibrous component, typically associated with collagen. The absence of experimental data in the axial direction required making assumptions for two of the model parameters determining the anisotropicity of the wall tissue: the fibre orientation parameter, α, and the fibre dispersion parameter, ρ (Haskett et al., 2010; Weisbecker et al., 2012). Previous studies showed that the human thoracic aorta exhibits a quasi-isotropic behaviour in young and middle-age donors, and tends to become stiffer axially than circumferentially in older adults (Haskett et al., 2010; Weisbecker et al., 2012). Therefore, in a first analysis, we assigned age-dependent values to α and ρ based on literature data and on the donor's age. Then, we repeated the analysis using age-independent values of α and ρ to assess whether our choice affected age-trends of the remaining parameters. Independently of the modelling choices for the anisotropy parameters, the elastin stiffness-like parameter μ was highest in the <30 years age group and significantly dropped by ~ 27–31% at 30–39 years with little further change thereafter (Figs. 4A and 5A). Conversely, changes in collagen exponential parameter, affecting the wall behaviour at high stresses, were observed with older age (≥ 60 years), nearly concomitant with the observed increase in $\dot{\mathscr{K}}_{\theta\theta\theta\theta}$. This result was also independent of fitting protocol (i.e., age-dependent/independent α and ρ).

Our constitutive modelling results are in agreement with previous empirical observations of age-related microstructural changes of the human aorta. For example; age trends of μ found in our study match well the drop in elastin density of the human thoracic aorta assessed via histological images of the wall cross-section in Jadidi et al. (2020). Further, in this work, differences in average stress-strain relationships between the <30, 30–39 and 40–49 years age-groups are consistent with the observation that elastase treatment (i.e., digestion of the elastin matrix) affects the shape of the stress-strain relationship of arteries at all stresses (Fonck et al., 2007). Indeed, the average stress-strain relationships of the age groups 30–39 and 40–49 years are consistently lower than that of the youngest age group (<30 years), Fig. 1B. Furthermore, the increase in the fibre non-linearity parameter found in our work possibly reflects the known enhanced collagen synthesis and increased cross-linking in older individuals (Graham et al., 2010; Harvey et al., 2016; Kohn et al., 2015; Tsamis and Stergiopulos, 2007). Therefore, we extrapolate the results of our constitutive modelling to suggest that elastin degradation and collagen remodelling with age may follow different time courses; the former occurring in young adults and the latter from middle-age onwards, possibly in response to the altered distribution of stresses within the wall that arise as a consequence of the first. Overall, despite the agreement between the results of the constitutive model used herein with those of other investigators, and due to the interdependence of its parameters, the interpretation of the results pertaining the changes in aortic microstructure needs to be taken with caution, given the absence of imaging or histological data.

Several mathematical descriptions of the behaviour of the human arterial wall constituents have been proposed previously (Haskett et al., 2010; Jadidi et al., 2020; Zulliger and Stergiopulos, 2007), and showed good ability in describing the macroscopic wall's mechanical response. The modelling performed in this work is based on a sizable human thoracic aorta empirical data. However, our experiments were conducted *ex vivo* and some of the model parameters may not match the behaviour of the wall constituents *in vivo*. Further, given the lack of experimental data in the axial direction, the modelling choices for α and ρ might have affected the outcomes of the analysis. The collagen stiffness-like parameter k_1 was the only parameter largely affected by the modelling assumptions; indeed, while k_1 negatively correlated with age when α and ρ were assumed constant for all age-groups, the former increased quadratically when using age-specific α and ρ. This result is not surprising when considering that α determines the relative and absolute contribution of collagen in the circumferential and axial direction. Therefore, as observed in the 60–69 and ≥ 70 years groups (Table 3), shifting the fibre orientation towards the axial direction (i.e., higher values of α) requires higher values of μ, k_1 and/or k_2 to attain the same circumferential response (Supplementary Fig. S1). Nevertheless, the exponential parameter k_2 dominates the response of the fibrous component of the SEF, so that observed differences in the age-trends of k_1 do not change the overall message of the constitutive modelling analysis.

The function of large arteries consists of transforming the pulsatile blood flow generated by the heart into a continuous flow. Arteries conduct this function by distending in systole to accommodate a high volume of blood and store elastic energy to be used in diastole to push the blood downstream in the circulation. In order to assess the impact of ageing on aortic function, we quantified the elastic energy per unit volume stored during pressurisation from 80 to 100 mmHg. Results suggested that wall remodelling successfully preserved aortic function until the age of 50–60; in the first four considered age-groups changes in $\Delta\Psi_{100-80\ \mathrm{mmHg}}$ were small. Conversely, $\Delta\Psi_{100-80\ \mathrm{mmHg}}$ started declining at the age of ~60 years and the physiological elastic function of the thoracic aorta was reduced by 56% over the investigated age range. These results are in agreement with previous findings (Jadidi et al., 2020) and explain the increase in pulse pressure observed in elastic arteries with age (Gurven et al., 2012; Shimura and Kubo, 2019; Wang et al., 2019).

4.1. Limitations

In this study, the mechanical properties of the human thoracic aorta have been evaluated *via* ring test, hence assessing the wall response to deformation in the circumferential direction only. This choice was dictated by the necessity of preserving the samples' integrity and limiting the amount of tissue required for the experiments. *In vivo*, the thoracic aorta is subjected to a complex mechanical loading configuration, that involves the superimposition of cyclic circumferential deformation and a constant axial stretch and that undoubtedly affects the aortic wall structure in more than one direction. Hence, biaxial testing may lead to a more thorough characterisation of the wall behaviour with ageing and elevated pressure levels, although the results of the current work are in line and good agreement with those reported by Jadidi et al. (2020) who also tested human aortas but using biaxial extension (see Figure 7 in Jadidi et al. (2020) and Fig. 1 here).

In this study, constitutive modelling was used to infer changes in wall

microstructure with age; namely, changes in the contribution of collagen and elastin to the wall mechanical behaviour. While the results reported here are in agreement with previous studies, confirming these through histological data would have strengthen the validity of the study. Unfortunately, these data were not acquired in this study, warranting further investigation to confirm our results.

5. Conclusions

This study showed that the human thoracic aorta undergoes significant stiffening during its life-course. The stiffening is further accentuated by increasing pressure levels. Constitutive modelling of the wall behaviour suggested that elastin and collagen follow different degeneration time-courses; the fragmentation of the elastin begins during the 3rd-4th decades (~30–40 years), then followed by increased stiffness of the collagen fibre network in late adulthood and old age (~50–60 years). These changes of the wall constituents impact the compliant function of the aorta, with its elastic properties declining from the 6th-7th decades (~60 years) onward.

CRediT authorship contribution statement

Alessandro Giudici: Writing – original draft, Methodology, Formal analysis, Data curation, Conceptualization. **Ye Li:** Project administration, Methodology, Investigation, Data curation. **Yasmin:** Project administration, Methodology, Investigation, Data curation, Project administration, Methodology, Investigation, Data curation. **Sarah Cleary:** Project administration, Data curation. **Kathleen Connolly:** Project administration, Data curation. **Carmel McEniery:** Writing – review & editing, Supervision, Project administration, Conceptualization. **Ian B. Wilkinson:** Writing – review & editing, Supervision, Project administration, Conceptualization. **Ashraf W. Khir:** Writing – review & editing, Supervision, Project administration, Conceptualization.

Declaration of competing interest

The authors declare that they have no known competing financial interests or personal relationships that could have appeared to influence the work reported in this paper.

Data availability

Data will be made available on request.

Appendix A. Supplementary data

Supplementary data to this article can be found online at https://doi.org/10.1016/j.jmbbm.2022.105339.

References

Bergel, D.H., 1961. The static elastic properties of the arterial wall. J. Physiol. 156, 445–457.

Burton, A.C., 1954. Relation of structure to function of the tissues of the wall of blood vessels. Physiol. Rev. 34, 619–642.

Cox, R.H., 1983. Comparison of arterial wall mechanics using ring and cylindrical segments. AJP - Hear. Circ. Physiol. 244, H298–H303.

Fonck, E., Prod'hom, G., Roy, S., Augsburger, L., Rüfenacht, D.A., Stergiopulos, N., 2007. Effect of elastin degradation on carotid wall mechanics as assessed by a constituent-based biomechanical model. Am. J. Physiol. Heart Circ. Physiol. 292, 2754–2763.

Franchini, G., Breslavsky, I.D., Holzapfel, G.A., Amabili, M., 2021. Viscoelastic characterization of human descending thoracic aortas under cyclic load. Acta Biomater. 130, 291–307.

Gasser, T.C., Ogden, R.W., Holzapfel, G.A., 2006. Hyperelastic modelling of arterial layers with distributed collagen fibre orientations. J. R. Soc. Interface 3, 15–35.

Giudici, A., Khir, A.W., Szafron, J.M., Spronck, B., 2021. From uniaxial testing of isolated layers to a tri-layered arterial wall: a novel constitutive modelling framework. Ann. Biomed. Eng. 49, 2454–2467.

Graham, Akhtar, Kridiotis, Derby, Kundu, Trafford, Sherratt, 2011. Localised micro-mechanical stiffening in the ageing aorta. Mech. Ageing Dev. 132, 459–467.

Graham, H.K., Hodson, N.W., Hoyland, J.A., Millward-Sadler, S.J., Garrod, D., Scothern, A., Griffiths, C.E.M., Watson, R.E.B., Cox, T.R., Erler, J.T., Trafford, A.W., Sherratt, M.J., 2010. Tissue section AFM: in situ ultrastructural imaging of native biomolecules. Matrix Biol. 29, 254–260.

Greenwald, S.E., 2007. Ageing of the conduit arteries. J. Pathol. 211, 157–172.

Gundiah, N., Babu, A.R., Pruitt, L.A., 2013. Effects of elastase and collagenase on the nonlinearity and anisotropy of porcine aorta. Physiol. Meas. 34, 1657–1673.

Gurven, M., Blackwell, A.D., Rodríguez, D.E., Stieglitz, J., Kaplan, H., 2012. Does blood pressure inevitably rise with age?: longitudinal evidence among forager-horticulturalists. Hypertension 60, 25–33.

Harvey, A., Montezano, A.C., Lopes, R.A., Rios, F., Touyz, R.M., 2016. Vascular fibrosis in aging and hypertension: molecular mechanisms and clinical implications. Can. J. Cardiol. 32, 659–668.

Haskett, D., Johnson, G., Zhou, A., Utzinger, U., Vande Geest, J., 2010. Microstructural and biomechanical alterations of the human aorta as a function of age and location. Biomech. Model. Mechanobiol. 9, 725–736.

Holzapfel, G.A., Ogden, R.W., 2010. Modelling the layer-specific three-dimensional residual stresses in arteries, with an application to the human aorta. J. R. Soc. Interface 7, 787–799.

Jadidi, M., Habibnezhad, M., Anttila, E., Maleckis, K., Desyatova, A., MacTaggart, J., Kamenskiy, A., 2020. Mechanical and structural changes in human thoracic aortas with age. Acta Biomater. 103, 172–188.

Kohn, J.C., Lampi, M.C., Reinhart-King, C.A., 2015. Age-related vascular stiffening: causes and consequences. Front. Genet. 6, 112.

Krasny, W., Morin, C., Magoariec, H., Avril, S., 2017. A comprehensive study of layer-specific morphological changes in the microstructure of carotid arteries under uniaxial load. Acta Biomater. 57, 342–351.

Learoyd, B.M., Taylor, M.G., 1966. Alterations with age in the viscoelastic properties of human arterial walls. Circ. Res. 18, 278–292.

Li, Y., Giudici, A., Wilkinson, I.B., Khir, A.W., 2021. Towards the non-invasive determination of arterial wall distensible properties: new approach using old formulae. J. Biomech., 110102

Peña, J.A., Martinez, M.A., Peña, E., 2015. Layer-specific residual deformations and uniaxial and biaxial mechanical properties of thoracic porcine aorta. J. Mech. Behav. Biomed. Mater. 50, 55–69.

Saini, A., Berry, C., Greenwald, S., 1995. The effect of age and sex on residual stress. J. Vasc. Res. 32, 398–405.

Shimura, K., Kubo, A., 2019. Characteristics of age-related changes in blood pressure, oxyhemoglobin saturation, and physique in Bolivians residing at different altitudes: presentation of basic data for health promotion. J. Phys. Ther. Sci. 31, 807–812.

Spina, M., Garbisa, S., Hinnie, J., Hunter, J.C., Serafini-Fracassini, A., 1983. Age-related changes in composition and mechanical properties of the tunica media of the upper thoracic human aorta. Arterioscler. Thromb. Vasc. Biol. 3, 64–76.

Spronck, B., Ferruzzi, J., Bellini, C., Caulk, A.W., Murtada, S.-I., Humphrey, J.D., 2020. Aortic remodeling is modest and sex-independent in mice when hypertension is superimposed on aging. J. Hypertens. 38, 1312–1321.

Tesauro, M., Mauriello, A., Rovella, V., Annicchiarico-Petruzzelli, M., Cardillo, C., Melino, G., Di Daniele, N., 2017. Arterial ageing: from endothelial dysfunction to vascular calcification. J. Intern. Med. 281, 471–482.

Tsamis, A., Krawiec, J.T., Vorp, D.A., 2013. Elastin and collagen fibre microstructure of the human aorta in ageing and disease: a review. J. R. Soc. 10, 1–22.

Tsamis, A., Stergiopulos, N., 2007. Arterial remodeling in response to hypertension using a constituent based model. Am. Physiol. Soc. 293, H3130–H3139.

Wang, R., Vetrano, D.L., Liang, Y., Qiu, C., 2019. The age-related blood pressure trajectories from young-old adults to centenarians: a cohort study. Int. J. Cardiol. 296, 141–148.

Weisbecker, H., Pierce, D.M., Regitnig, P., Holzapfel, G.A., 2012. Layer-specific damage experiments and modeling of human thoracic and abdominal aortas with non-atherosclerotic intimal thickening. J. Mech. Behav. Biomed. Mater. 12, 93–106.

Wolinsky, H., Glagov, S., 1964. Structural basis for the static mechanical properties of the aortic media. Circ. Res. 14, 400–413.

Zulliger, M.A., Stergiopulos, N., 2007. Structural strain energy function applied to the ageing of the human aorta. J. Biomech. 40, 3061–3069.